EXPERIMENTAL STUDY OF DYNAMIC THERMAL BEHAVIOUR OF AN 11 KV DISTRIBUTION TRANSFORMER

Rafael VILLARROEL
The University of Manchester - UK
rafael.villarroelrodriguez@manchester.ac.uk

Qiang LIU
The University of Manchester - UK
qiang.liu@manchester.ac.uk

Zhongdong WANG
The University of Manchester - UK
zhongdong.wang@manchester.ac.uk

ABSTRACT

This paper investigates the dynamic thermal behaviour of a 200 kVA, 11/0.433 kV mineral oil filled and oil natural–air natural (ONAN) cooled distribution transformer manufactured with 16 fibre optic sensors inside the tank. The transformer was subjected to extended temperature rise tests under multiple levels of constant loadings, i.e. 0.7 pu, 1.0 pu and 1.25 pu to derive the thermal parameters required in the IEC thermal model for estimating the hot-spot temperature (HST). Measured and estimated HSTs are compared through a validation test simulating a short period overloading up to 1.8 pu for 2 hours. Based on the data availability, three scenarios or cases are proposed to derive thermal parameters. Thermal parameters derived based the internal fibre optic sensor measurements provide the best estimation of HST.

INTRODUCTION

Reliability of transformers is essential for the safe operation of distribution networks. One of the main failure mechanisms of distribution transformers is bubble formation under overheated conditions, which is predominately determined by the hot-spot temperature (HST) inside the transformer. In addition, HST is essential to estimate the life expectancy of transformer insulation system [1].

The dynamic thermal rating (DTR) of distribution transformers requires understanding the thermal behaviour of transformers under dynamic load scenarios. The key to DTR is to estimate the HST, based on which the rating of transformer can be optimised responsively and predictably.

The HST is described as the sum of the ambient temperature, the top-oil temperature rise and the hot-spot-to-top-oil gradient in IEEE C57.91 [2]. It should be referred to the adjacent top-oil temperature inside the winding [3], where the oil temperature increases linearly from bottom to top and the temperature of the winding rise is parallel to the oil temperature rise, with a constant difference g_r between the two straight lines [3].

Fibre optic sensors have been widely used to measure temperature distribution and the HST for power transformers [4, 5]. In this work, the same technique is used to carry out a set of temperature rise tests for an 11 kV distribution transformer, where different cases of available information are proposed to analyse their effect on the HST derivation. Referring to the IEC thermal model [3], a set of new thermal parameters are then determined based on the experimental results. An additional test simulating a short period overloading is undertaken to verify the newly derived thermal parameters.

TESTED TRANSFORMER

The transformer used in this work is a 200 kVA, 11/0.433 kV distribution transformer with ONAN cooling mode and filled with mineral oil. It has been specially manufactured with 16 fibre optic temperature sensors embedded into different locations carefully chosen in order to capture the HST and the top and bottom oil temperatures inside the tank.

EXPERIMENTAL DESCRIPTION

A set of extended temperature rise tests on the transformer were carried out according to IEC 60076-2 [6], where the short-circuit method was used .

Experimental Setup

The short-circuit method followed the procedure specified in IEC Standard 60076-2 [6]. During the test, the LV terminals of the transformer were short-circuited using a solid copper link, and the transformer is then subjected to a test current corresponding to the calculated total losses (load losses plus no-load losses) [7]. A schematic diagram of the experimental setup is shown in Figure 1.

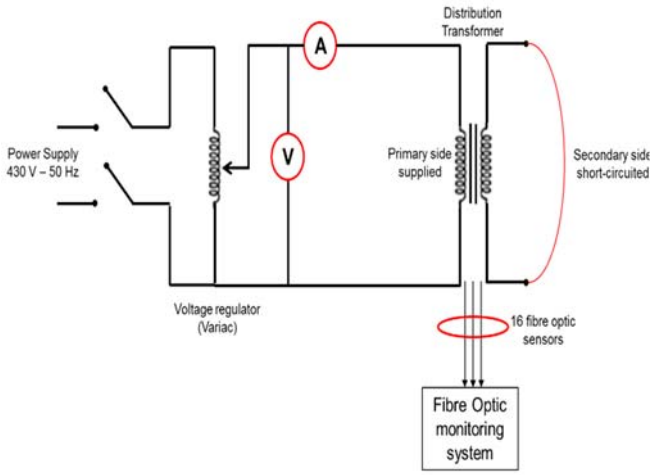

Figure 1. Experimental setup of temperature rise tests.

Top oil temperatures were measured by thermocouples at the oil pocket on the top of the transformer and top of the radiator (upper tube to the radiator), whereas bottom oil temperature at the bottom of the radiator (lower tube to the radiator).

In addition to the thermocouples placed outside of the tank, temperatures inside the transformer were measured by fibre optic sensors installed at the top of the LV and HV windings to register the HST as well as sensors installed in a Bakelite frame next to the inlet and outlet of the radiator to measure the top and bottom temperatures.
Ambient temperature around the transformer was also measured by four thermocouples immersed in small oil-filled containers at 1 m high from ground and at a distance of 2 m from each side of the transformer according to [6], and the average of their readings is used for the evaluation of the ambient temperature.

Extended Temperature Rise Tests

The steady state oil temperature rise at top and bottom of the transformer as well as the average winding temperatures are measured at constant load profiles of 0.7 pu, 1.0 pu and 1.25 pu according to IEC 60076-2 [6].
At the beginning of the test, the transformer is subjected to a test current corresponding to the total losses (load losses plus no-load losses) at the 1.0 pu, until reaching the steady state, where the rate of change of top-oil temperature rise had fallen below 1 K/h and remained there for a period of 3 hours. In the second step, the test current is reduced to the current corresponding to the load losses for a duration of 1 hour. In the final step, the load supply is disconnected, and the average winding resistance measurement starts.
The average winding temperatures are determined from the continuous resistance measurements. Due to the Winding resistance value decreases with time, measurements must be extrapolated backwards in time to the instant of shutdown to obtain the winding resistance value at that time.
The duration of the winding resistance cooling down curve should be at least two times the thermal time constant of the winding [6], then the total duration of the measurements was 30 minutes, according to the characteristics of the transformer used, and measurements were taken in intervals of 15 seconds.
The procedure applied to 1.0 pu load profile was repeated to 0.7 pu and 1.25 pu load profiles to complete the extended temperature rise tests.

EXPERIMENTAL RESULTS

The hottest temperature was always measured at the top of the LV winding in phase A, furthest away from the radiator, from a total of eight sensors distributed at the top of HV and LV windings. The dynamic profiles of HST recorded during the extended temperature rise tests at 0.7 pu, 1.0 pu and 1.25 pu are shown in Figure 2.
Top-oil temperatures were measured at different locations inside and outside the transformer tank. Measurements at internal top oil give the highest values followed by oil pocket and then external top oil.
Bottom-oil temperatures were also recorded at internal and external locations, where measurements at internal bottom oil give higher values than those at external bottom oil.

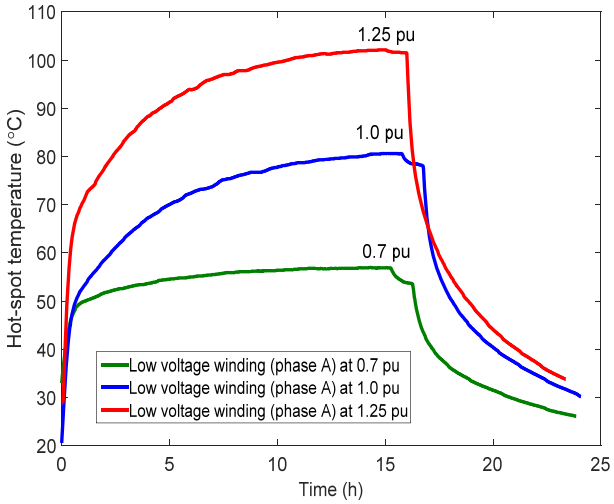

Figure 2. Hotspot temperature in low voltage windings (phase A) at different constant load profiles.

Table 1 summarises the measured temperatures at the oil pocket, internal top oil and bottom oil, external top oil and bottom oil, hotspot at the LV winding in phase A and ambient, which are used in this work to derive the thermal parameters.

Table 1. Absolute temperatures in °C from temperature rise tests.

Temperature	0.7 pu	1.0 pu	1.25 pu
Average ambient	18.8	17.6	18.3
HST (LV phase A)	56.9	80.6	102.0
Internal top oil	44.4	60.3	76.5
Internal bottom oil	35.9	50.4	65.0
Oil pocket	40.9	55.2	69.8
External top oil	37.8	51.0	63.9
External bottom oil	33.3	46.2	59.7

IEC THERMAL MODEL

The thermal model in standard IEC 60076-7 [3] was adopted to estimate the HST. It considers the HST as a function of time, for varying load current and ambient temperature. Therefore, a HST corresponding to a load factor of K is given by Equation 1 [3].

$$\theta_h(t) = \theta_a + \Delta\theta_{o(i)} + \left\{ \Delta\theta_{or} \times \left[\frac{1+R\times K^2}{1+R} \right]^x - \Delta\theta_{o(i)} \right\} \times f_1(t) + A$$

Equation 1

Where:

$$A = \Delta\theta_{h(i)} + \left\{ H \times g_r \times K^y - \Delta\theta_{h(i)} \right\} \times f_2(t)$$

$$f_1(t) = \left(1 - e^{(-t)/(k_{11}\times\tau_o)}\right)$$

$$f_2(t) = k_{21} \times \left(1 - e^{(-t)/(k_{22}\times\tau_w)}\right) - \left(k_{21} - 1\right) \times \left(1 - e^{(-t)/(\tau_o/k_{22})}\right)$$

Function $f_1(t)$ describes the increase of the top-oil temperature rise according to the unit of the steady-state value, while $f_2(t)$ describes the relative increase of the hot-spot-to-top-oil gradient. Parameters required to implement Equation 1 are: thermal model constants k_{11}, k_{21} and k_{22} which are given in [3]; θ_h is the HST, θ_a is the ambient temperature, $\Delta\theta_o$ and $\Delta\theta_{or}$ are the top-oil temperature rise in steady state at the load considered and at rated losses, respectively, $\Delta\theta_h$ is the hot-spot-to-top-oil gradient at the load considered, K is the load factor used during the tests, R is the ratio of load losses at rated current to no-load losses obtained from routine tests, H is the hot-spot factor, and g_r is the average-winding-to-average-oil temperature gradient at rated current. Oil exponent (x), winding exponent (y), oil time constant (τ_o) and winding time constant (τ_w) are thermal parameters to be determined by implementation of the differential equations solution method proposed in [3].

DERIVATION OF THERMAL PARAMETERS

To study the effect of the locations of the sensors on the estimation of the HST, three different scenarios/cases are proposed to derive thermal parameters. Cases proposed and studied in this work are given as follows:

- Case 1 is based on the estimation of the HST using thermal parameters proposed in the standard IEC 60076-7 [3]. This case represents the scenario that temperature rise test results are not available. Therefore it uses conservative values, i.e. the temperature rise limit required in IEC 60076-2 [6], top-oil temperature rise of 60 K over ambient temperature and HST rise of 18 K over top oil temperature.

- Case 2 estimates the HST using derived thermal parameters from temperature rise tests based on external temperature measurements, therefore values at the top and bottom of the radiator pipe and oil pocket are used to estimate the top oil temperature and the average oil temperature. HST is not directly measured in this case, so it is then derived from the hot-spot-factor (HSF) of 1.1 suggested for distribution transformers [3]. This case is commonly used in factory when internal fibre optic sensors are not available.

- Case 3 estimates the HST using derived thermal parameters from measured temperatures inside the transformer based on fibre optic sensors. HST is directly measured by fibre optic sensors inside the winding. This case is not frequently used in factory due to the complexity and cost of the fibre optic sensors installation. However, it seems necessary in terms of understanding a specific thermal design and corresponding thermal parameters.

Oil time constant (τ_o)

As it is mentioned in [8], the oil time constant can be derived by curve fitting of the top oil temperature rise. Figure 3 shows the top oil temperature rise and exponential fitting curves for cases 2 and 3 proposed in this work, to determine the oil time constant at 1.0 pu load profile. Oil time constant for case 1 is taken from IEC 60076-7 [3]. Oil time constant values obtained are: case 1 =180 min (taken from [3]), case 2=216 min and case 3=244 min.

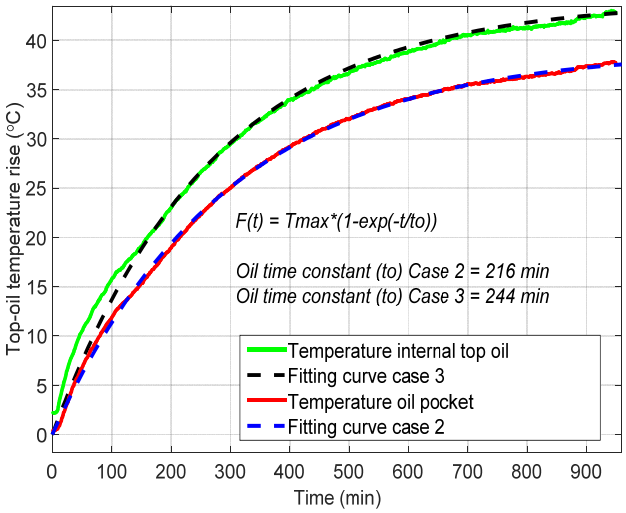

Figure 3. Fitting top oil temperature rise from internal fibre optic sensor and oil pocket at 1.0 load factor.

Winding time constant (τ_w)

A numerical extrapolation method of cooling down curve proposed in [6] was used to determine the winding time constant. This method can be used to fit an analytical function to a set of timewise equidistant temperature readings. The winding time constants (τ_w) were then calculated for both cases 2 and 3 based on the average oil temperature from thermocouples/fibre optic sensors placed at the aforementioned locations as well as the average winding resistance measurements. Winding time constant values obtained are: case 1=4 min (taken from [3]), case 2=9.6 min and case 3=9.4 min.

Oil exponent (x):

According to IEC 60076-7 [3] when the transformer reaches the steady state, the top-oil temperature rise can be determined by the Equation 2 [3]:

$$\Delta\theta_o = \left[\frac{1+R\times K^2}{1+R}\right]^x \times \Delta\theta_{or}$$

Equation 2

R and $\Delta\theta_o$ are obtained from routine test and extended temperature rise tests respectively, then the oil exponent (x) can be obtained by plotting the ratio of $\Delta\theta_o/\Delta\theta_{or}$ against the value of $\left[\frac{1+R\times K^2}{1+R}\right]$ in a log-log plot. Derivation of (x)

is shown in Figure 4, where values correspond to the slope of the straight line that best fits all points. Oil exponent values are: case 1=0.80 (taken from [3]), case 2=0.82 and case 3=0.79.

Winding exponent (*y*):

The winding exponent *(y)* can be also derived from steady state conditions by plotting the ratio of the average winding resistance under a load factor (*K*) and the average winding resistance at rated load factor against the load factor in a log-log plot according to the Equation 3 [3].

$$g = g_r \times K^y$$

Equation 3

In the same way, derivation of *(y)* is shown in Figure 5, where values correspond to the slope of the straight line that best fits all points. Oil exponent values are: case 1=1.6 (taken from [3]), case 2=1.4 and case 3=1.5.

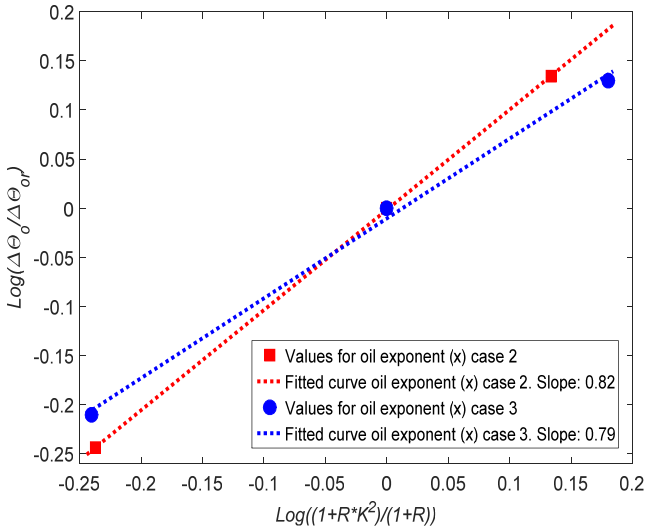

Figure 4. Derivation of the oil exponent *(x)* for cases 2 and 3.

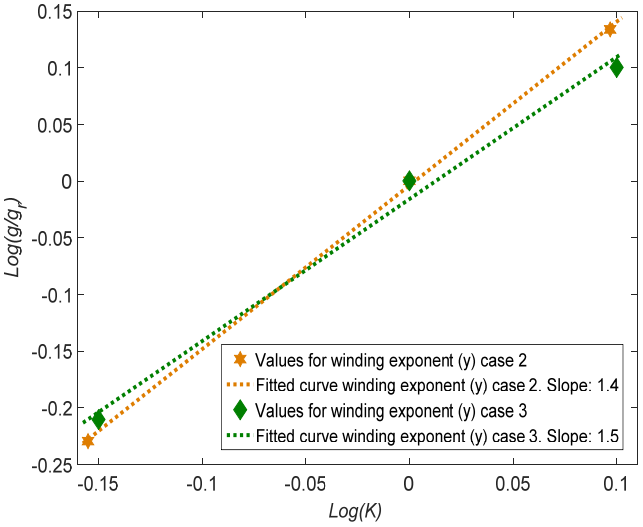

Figure 5. Derivation of the winding exponent *(y)* for cases 2 and 3.

As results of this section, Table 2 summarises all thermal parameters derived from the extended temperature rise tests and proposed in IEC 60076-7 [3] for the three cases proposed in this work. Key parameters such as $\Delta\theta_{or}$, the hot-spot-to-top-oil gradient at rated current $(\Delta\theta_{hr})$ and g_r are obtained from the temperature rise tests for both case 2 and case 3. *H* is taken as the ratio of the $\Delta\theta_{hr}$ to g_r for case 3, which is 1.5. While HST measurements are not available for case 1 and case 2, *H* of 1.1 is used according to IEC 60076-7 [3].

Table 2. Summary of thermal parameters for three case studies.

Parameters	Case 1	Case 2	Case 3
$\Delta\theta_{or}$ *(K)*	60.0	37.6	42.7
$\Delta\theta_{hr}$ *(K)*	18.0	17.7	20.3
x	0.80	0.82	0.79
y	1.6	1.4	1.5
$\tau_{o\ (min)}$	180	216	244
$\tau_{w\ (min)}$	4.0	9.6	9.4
g_r	16.4	16.1	13.6
H	1.1	1.1	1.5

EXPERIMENTAL VALIDATION

Thermal parameters derived in this work (Table 2) were validated by comparing the measured HST with the estimated one in a validation test which represents a short period overloading scenario. It is based on a two-step load profile where the transformer was subjected to 0.7 pu for 17 hours, 1.8 pu for 2 hours and 0.7 pu for 4 hours. Figure 6 shows a comparison of three estimated HSTs from the proposed cases and the measured HST using fibre optic sensors.

Root-mean-square-deviation *(rmsd)*

To quantify the difference between the experimental HST curve and the estimated curve, the calculation of the root-mean-square-deviation *(rmsd)* was done according to Equation 4, which has been used in previous works [9]. Where ***n*** is the number of readings, $\theta_{HS(estimated)}$ and $\theta_{HS(experimental)}$ are the estimated HST and the measured HST, respectively.

$$rmsd = \sqrt{\frac{1}{n}\sum_{i=1}^{n}\left[\theta_{HS(estimated)}(t_i) - \theta_{HS(experimental)}(t_i)\right]^2}$$

Equation 4

Values obtained for the three cases are: case 1=12.4, case 2=6.2 and case 3=2.2, which indicates case 3 provides the best estimation of HST.

From Figure 6 it can be noticed that the estimation obtained using thermal parameters from case 1 is far from the experimental data, where the HST reached a peak value of 155.1°C, overestimated by 32.6°C compared to the measured value. On the other hand, although the estimated HST using thermal parameters from case 2 fits better to the measured values than the one from case 1, it is underestimated by 10.3°C. The thermal parameters obtained from case 3 using internal fibre optic sensors provide the best estimation of HST with a maximum difference of 4°C.

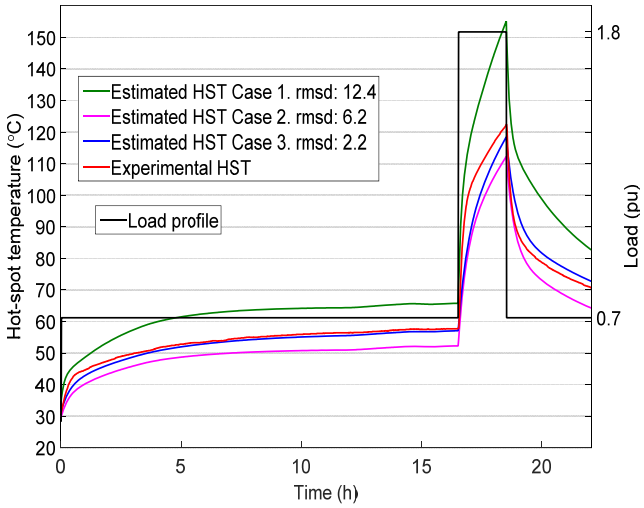

Figure 6. Comparison of the estimated HST using parameters from cases 1, 2 and 3 and the measured HST under a two-step overloading profile.

CONCLUSION

In this work a 200 kVA, 11/0.433 kV distribution transformer with built-in fibre optic sensors has been tested under different load scenarios to study its dynamic thermal rating. Extended temperature rise tests under three constant load profiles have been carried out on the transformer to derive thermal parameters needed to estimate the HST by implementing the IEC thermal model. Based on the data measured from internal and external sensors as well as values taken from the IEC standard, three different cases or scenarios have been proposed to analyse the thermal behaviour of the transformer. The HST was estimated and compared with experimental data obtained from an additional validation test based on a two-step load profile, where the transformer was subjected to a load peak value of 1.8 pu for 2 hours.

The HST was overestimated when thermal parameters referred to the IEC standard (Case 1) were used. Thermal parameters derived from external sensors (Case 2) underestimated the HST. The best estimation of the HST was achieved by implementing thermal parameters derived from internal sensors (Case 3). Comparing the three sets of thermal parameters, one of the key differences is oil time constant, which could be the major reason causing the different estimation of HST under short term overloading conditions.

Acknowledgments

This work was funded by the Engineering and Physical Sciences Research Council (EPSRC) through the Innovate UK consortium project “Common Application Platform for Low Voltage Network Management”, grant number EP/N508421/1.

Special thanks to Innovate UK and the industry partners EA Technology and Nortech for their contributions to this project.

The authors would also like to thank Winder Power for its valuable input on the construction of the transformer used in this work.

REFERENCES

[1] CIGRE, 2009, "Thermal performance of transformers," *Working Group A2.24. Technical Brochure 393,* vol. 129.

[2] IEEE C57.91, 2012, "Guide for Loading Mineral-Oil-Immersed Transformers and Step-Voltage Regulators," 1-123.

[3] IEC 60076-7, 2005, "Loading guide for oil-immersed power transformers," in *Power transformers–Part 7*.

[4] Z. Radakovic and K. Feser, 2003, "A new method for the calculation of the hot-spot temperature in power transformers with ONAN cooling," *Power Delivery, IEEE Transactions on,* vol. 18, 1284-1292.

[5] D. Susa and H. Nordman, 2009, "A simple model for calculating transformer hot-spot temperature," *IEEE transactions on power delivery,* vol. 24, 1257-1265.

[6] IEC 60076-2, 2011, "Temperature rise for liquid-immersed transformers" *Power transformers–Part 2*.

[7] IEC 60076-1, 2011, "General" *Power Transformers part 1*".

[8] Y. Gao, Z. Wang, and D. Jones, 2014, "How to make use of transformer heat run test results? review on thermal parameter derivation methods," in *International Conference on Condition Monitoring and Diagnosis (CMD),* 383-387.

[9] R. Villarroel, D. F. García, B. García, and J. C. Burgos, 2015, "Moisture diffusion coefficients of transformer pressboard insulation impregnated with natural esters," *IEEE Transactions on Dielectrics and Electrical Insulation,* vol. 22, 581-589.